

Polarization-anisotropy induced spatial anisotropy of polariton amplification in planar semiconductor microcavities

Stefan Schumacher

College of Optical Sciences, University of Arizona, Tucson, Arizona 85721, USA

(Dated: November 11, 2018)

Based on a microscopic many-particle theory we investigate the amplification of polaritons in planar semiconductor microcavities. We study a spatially perfectly isotropic microcavity system and excitation geometry. For this system, our analysis shows that a pump-induced vectorial polarization anisotropy can lead to a spatial anisotropy in the stimulated amplification of polaritons. This effect is brought about by the interplay of the longitudinal-transverse cavity mode splitting (TE-TM splitting) and the spin-dependence of the polariton-polariton scattering processes.

PACS numbers: 71.35.-y, 71.36.+c, 42.65.Sf, 42.65.-k

INTRODUCTION – In the past decade the parametric amplification of polaritons in planar semiconductor microcavities has been intensively investigated in theory and experiment, see, e.g., Refs. 1,2,3,4,5,6 or the reviews given in Refs. 7,8,9. Whereas the polariton amplification was initially reported in a co-circularly polarized pump-probe setup¹, for other configurations it can show a rich vectorial polarization dependence.^{10,11,12,13,14,15,16,17,18,19,20} This vectorial polarization dependence is governed by the underlying spin-dependent polariton-polariton scattering processes, longitudinal-transverse cavity mode splitting (TE-TM splitting), and possible structural anisotropy of the investigated systems.

In the most intensively studied configuration, a pump pulse induces a coherent polariton density close to the inflection point of the lower polariton branch (LPB), the so-called “magic angle”. In this configuration phase-matched resonant pairwise scattering of pump-induced polaritons into probe and four-wave mixing (FWM) directions is allowed which makes the polariton amplification most efficient. However, for oblique pump excitation the intrinsic cylindrical symmetry of the planar microcavity system is destroyed by the optical fields.

In this paper, we study an excitation geometry where the incoming pump does not necessarily spoil the symmetry of the system. As the simplest such configuration, we investigate the polariton amplification for excitation with a pump pulse, which is incident along the system’s symmetry axis, i.e., perpendicular to the plane of the embedded quantum well along the z axis. In this excitation configuration the pump-excited polaritons carry zero in-plane momentum $\mathbf{k}_p = 0$. As illustrated in Fig. 1, for pump frequency above the LPB, FWM processes triggered by fluctuations in the cavity photon field can give rise to pairwise off-axis scattering of pump-excited polaritons into two polaritons with finite and opposing in-plane momentum \mathbf{k} and $-\mathbf{k}$. For a pump-induced exciton density above the stimulated amplification threshold these scattering processes can lead to strong off-axis ($\mathbf{k} \neq 0$) signals as has been demonstrated in Ref. 21 for a slightly different excitation geometry. For the perfectly isotropic system studied in this work, spontaneous (fluctuation-

induced) off-axis pattern formation is expected which is invariant under rotation about the propagation direction of the pump.

Based on a microscopic many-particle theory we discuss that even if the incoming optical pump field does not destroy the spatial isotropy of the system, a specific choice of its vectorial polarization state can lead to a pronounced azimuthal angular dependence of the spontaneous signals in the off-axis directions. We discuss the interplay of the longitudinal-transverse cavity mode splitting (TE-TM splitting) and the spin-dependent polariton-polariton scattering processes that leads to this spatial anisotropy, solely induced by a vectorial polarization anisotropy.

MICROSCOPIC THEORY – Our theoretical analysis is based on the microscopic many-particle theory presented in Ref. 17. It includes spin and frequency dependent polariton-polariton scattering^{22,23,24,25} and a TE-TM cavity mode splitting in the coupled cavity-confined

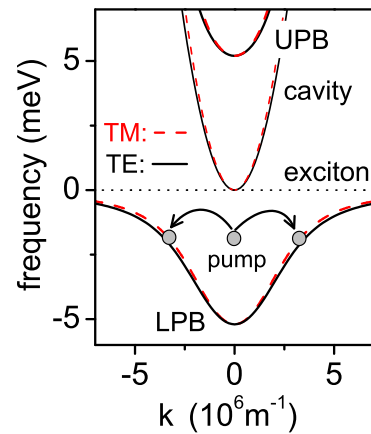


FIG. 1: (color online) Shown are the isotropic TE (solid) and TM (dashed) cavity polariton modes on the lower (LPB) and upper (UPB) polariton branch, respectively. Also shown are the bare cavity and exciton dispersions. The basic pairwise off-axis scattering of pump-induced polaritons is indicated. For the GaAs parameters used and for the modeling of the cavity dispersion see Ref. 17.

field and exciton dynamics. Calculations are done for the same GaAs based microcavity system studied in Ref. 17 but for a slightly smaller intrinsic dephasing for the excitonic polarization amplitude and the fields in the cavity modes, $\gamma_x = \gamma_c = 0.15$ meV. Within this framework and for steady-state monochromatic pump excitation with frequency ω_p , the linearized coupled dynamics for field and excitonic polarization components with in-plane momenta \mathbf{k} and $-\mathbf{k}$ can be cast into the following simple form:

$$\hbar \dot{\tilde{\mathbf{p}}}_{\mathbf{k}} = M_{\mathbf{k}} \tilde{\mathbf{p}}_{\mathbf{k}}. \quad (1)$$

The vector $\tilde{\mathbf{p}}_{\mathbf{k}}$ groups together the dynamic variables for field components (in the TE and TM cavity modes, respectively) and excitonic polarization components (longitudinal or transversal to \mathbf{k} , respectively). Analyzing the linear stability of the pump-driven polariton dynamics against off-axis fluctuations, no incoming fields in the \mathbf{k} and $-\mathbf{k}$ directions are explicitly considered. The matrix $M_{\mathbf{k}}$ is a \mathbf{k} -dependent but time independent matrix where all the system and pump parameters enter. The components of $\tilde{\mathbf{p}}_{\mathbf{k}}$ carry only the time dependence relative to the time dependence $\sim e^{-i\omega_p t}$ that is imposed by the pump field. This additional time dependence is determined by the eigenvalues λ of $M_{\mathbf{k}}$. The two-exciton continuum is treated in Markov approximation as in Ref. 17 but non-Markovian contributions from excitation of the bound biexciton state are included in Eq. (1). This Markov approximation should be particularly well fulfilled for the present study since the dominant and thus relevant modes oscillate with or close to the pump frequency ω_p (cf. Fig. 1). We neglect the influence of excitonic phase-space filling nonlinearities which have been found to be insignificant for the stimulated polariton amplification.¹⁷ To concentrate on the issues under investigation, we do not consider possible complications of our discussion from bistability²⁶ or multistability²⁷ for the steady-state pump-induced polarization.

Within this framework, the eigenvalues λ of $M_{\mathbf{k}}$ contain comprehensive information about temporal growth or decay (real part of λ) and frequency (imaginary part of λ) of the possible off-axis modes as long as the system dynamics is linear in the off-axis contributions. Information about the vectorial polarization state of these modes is contained in the respective eigenvectors. We investigate the system dynamics for a total (including both vectorial polarization states) pump-induced exciton density of $5 \cdot 10^9 \text{ cm}^{-2}$, which is close to the amplification threshold, and pump frequency ω_p tuned 2 meV below the bare exciton resonance. The data presented in the following quantitatively depend on the choice of excitation, cavity and other material parameters. However, the qualitative nature of the results is robust. We diagonalize $M_{\mathbf{k}}$ for different in-plane momenta \mathbf{k} , and analyze the real-part of the eigenvalue λ with the largest real part. This gives us the growth rate of the initially fastest growing and therefore “most unstable” mode, which will eventually dominate the system dynamics for sufficiently long

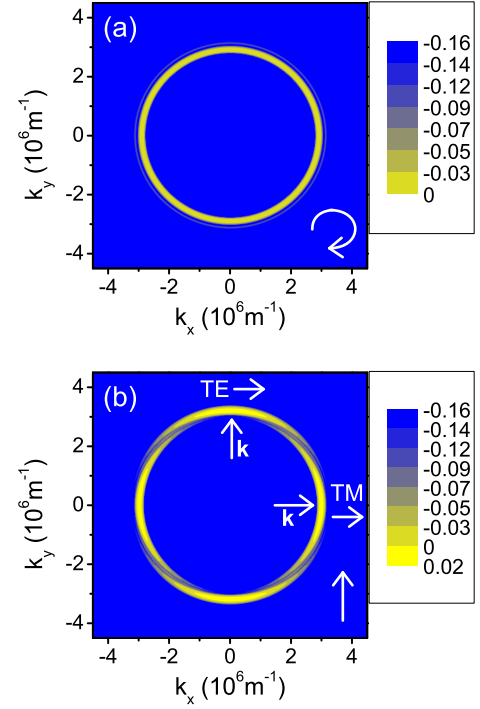


FIG. 2: (color online) Maximum growth rate for signals with in-plane momenta \mathbf{k} and $-\mathbf{k}$. Results are given in meV and the vectorial pump polarization state is indicated in the lower right corner of each panel. Results are calculated including TE-TM cavity-mode splitting and excitonic correlations. (a) Circularly polarized pump. The off-axis scattering is isotropic. (b) Linearly polarized pump. The preferred vectorial polarization state for the signals scattered off-axis ($\mathbf{k} \neq 0$) is perpendicular to the pump’s polarization vector. For \mathbf{k} parallel (perpendicular) to the pump’s polarization vector, scattering in the TE (TM) mode is preferred. The momentum \mathbf{k} and the preferred polarization vector for the scattered signals is indicated for \mathbf{k} parallel and perpendicular to the pump’s polarization vector, respectively. Together with the TE-TM mode splitting, this polarization dependence leads to the spatial anisotropy in the off-axis signals.

growth periods.

RESULTS AND DISCUSSION – For excitation with a circularly polarized pump, Fig. 2(a) shows the real-part of the eigenvalue λ of $M_{\mathbf{k}}$ with the largest real part, i.e., the maximum growth (for $\text{Re}\{\lambda\} > 0$) or minimum decay (for $\text{Re}\{\lambda\} < 0$) rate for each \mathbf{k} . (In the following loosely referred to as ‘growth’.) The largest growth rate is found on the ‘elastic circle’ where pairs of the off-resonantly excited pump polaritons can resonantly be scattered on the pump-renormalized polariton dispersion (cf. Fig. 1). No angular dependence of the displayed growth rates, and thus no anisotropy of the stimulated scattering is found. Note that for the chosen pump density the stimulated amplification threshold is not reached (all $\text{Re}\{\lambda\} < 0$) in Fig. 2(a), all modes are exponentially decaying and no significant off-axis scattering of light initiated by fluctuations is expected.

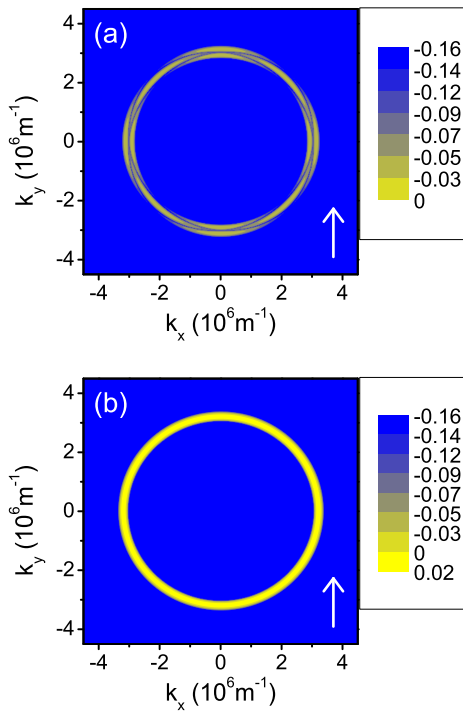


FIG. 3: (color online) (a) Same as Fig. 2(b) but evaluated on the mean-field Hartree-Fock level neglecting excitonic correlations. (b) Same as Fig. 2(b) but without TE-TM cavity-mode splitting. (a), (b) The vectorial pump polarization state is indicated in the lower right corner of each panel.

This situation changes for excitation with a linearly polarized pump as shown in Fig. 2(b). By choosing a particular orientation of the vectorial polarization of the pump, the spin-dependent polariton-polariton scattering together with the TE-TM cavity mode splitting induces a spatial anisotropy for the growth of off-axis signals over time. It is worthwhile to emphasize again that this anisotropy comes about without any anisotropy in the cavity or the quantum well. The stimulated scattering intrinsically depends on the orientation of \mathbf{k} to the pump's linear polarization vector: Owing to the spin-dependence of the underlying polariton-polariton scattering processes, polaritons scattered off-axis are preferably polarized perpendicular to the pump's vectorial polarization state.¹⁷ This preference leads to different scattering rates into the TE or TM polarized modes, depending on the orientation of the off-axis momenta \mathbf{k} and $-\mathbf{k}$ of the scattered polaritons relative to the pump's polarization vector. For the TE mode, the electric field vector is perpendicular to the plane of incidence, thus also perpendicular to \mathbf{k} . For the TM mode, the component of the electric field vector in the quantum well plane is parallel to \mathbf{k} . Therefore, for the results shown in Fig. 2(b), for \mathbf{k} parallel to the pump's polarization vector, scattering in the TE mode is preferred. For \mathbf{k} perpendicular to the pump's polarization vector, scattering into the TM mode is preferred. A similar anisotropy has been ob-

served earlier but in the linear optical regime, in the ballistic propagation of cavity polariton wave packets²⁸ and in Ref. 29 where an optical spin Hall effect was proposed. In Refs. 28,29 the TE-TM cavity mode splitting has led to a four-fold rotation symmetry in the results. In our case the spin-dependent many-particle interactions reduce the rotation invariance further to a two-fold rotation symmetry. As shown in Fig. 3(a), a four-fold rotation symmetry in the polariton amplification can only be regained if the polariton-polariton scattering is treated on the mean-field Hartree-Fock level, neglecting excitonic correlations in the scattering processes. For scattering with \mathbf{k} either parallel or perpendicular to the pump's polarization vector, $M_{\mathbf{k}}$ in Eq. (1) is block-diagonal. Consequently, in these directions the polaritons are scattered off-axis either into the TE or into the TM mode. For all other orientations, the eigenvectors of $M_{\mathbf{k}}$ contain contributions from both TE and TM modes. Note that without correlations in Fig. 3(a) again the amplification threshold is not reached for the chosen density.

Finally, Fig. 3(b) shows the growth rate including correlations but for zero TE-TM cavity mode splitting. Circular symmetry is recovered and the amplification threshold is reached. This indicates that minimization or proper engineering of the TE-TM cavity-mode splitting – at least close to ω_p – can be used to rebuild the isotropy of the stimulated amplification mechanism. This way possible benefits of excitation with a linearly polarized pump, such as a lower threshold density or polarization-selective separation of the off-axis signals from the pump, respectively, may be accessible without inducing an undesired anisotropy in the system dynamics.

Strictly speaking, the linear stability analysis discussed above only reveals information about the initial growth of off-axis fluctuations as long as the system dynamics is linear in the resulting off-axis signals. To avoid a clear deviation from this situation in an experimental attempt to verify the discussed results, the pump frequency ω_p should be chosen such that the off-axis scattering of pump polaritons does not lead to a significant buildup of polariton density at the “magic angle”. This precaution is in analogy to Ref. 21 and prevents that polariton scattering at the “magic angle” would eventually take over the nonlinear system dynamics with increasing intensity of the off-axis signals over time.

As an alternative to the steady-state experiment, all assumptions entering the linear stability analysis can be well satisfied in a typical pump-probe experiment: The pump pulse needs to be long enough, so that the steady-state limit is imitated in a good approximation. The incoming probe pulse must be weak so that even after amplification it does not significantly influence the polarization dynamics in the pump direction. The incoming probe pulse should also be short enough so that it does not considerably drive the polarization dynamics, but merely acts as a seed for the off-axis signal in the probe direction. With the pump pulse in normal incidence, the probe pulse is used to map out the amplifica-

tion in the k_x, k_y plane.

REMARKS & CONCLUSIONS – We have shown that in a perfectly isotropic microcavity system a vectorial polarization anisotropy of the pump can induce a spatial anisotropy for the stimulated amplification of polaritons. This anisotropy is brought about by the combined influence of a TE-TM cavity mode splitting and the spin-dependent polariton-polariton scattering processes. Besides its general interest, this effect may have an influence on, e.g., the generation of correlated photon pairs in the

stimulated amplification regime.²¹ Angular dependencies as discussed in this work are also expected to play a role in other systems^{30,31} as long as they are not overshadowed by structural imperfections.

ACKNOWLEDGMENTS – The author gratefully acknowledges various fruitful discussions with Nai H. Kwong and Rolf Binder throughout this project. He also acknowledges support by the Deutsche Forschungsgemeinschaft (DFG, project No. SCHU 1980/3-1). This work has further been supported by ONR, DARPA, and JSOP.

-
- ¹ P. G. Savvidis, J. J. Baumberg, R. M. Stevenson, M. S. Skolnick, D. M. Whittaker, and J. S. Roberts, *Phys. Rev. Lett.* **84**, 1547 (2000).
 - ² R. Huang, F. Tassone, and Y. Yamamoto, *Phys. Rev. B* **61**, R7854 (2000).
 - ³ C. Ciuti, P. Schwendimann, B. Deveaud, and A. Quattropani, *Phys. Rev. B* **62**, R4825 (2000).
 - ⁴ R. M. Stevenson, V. N. Astratov, M. S. Skolnick, D. M. Whittaker, M. Emam-Ismael, A. I. Tartakovskii, P. G. Savvidis, J. J. Baumberg, and J. S. Roberts, *Phys. Rev. Lett.* **85**, 3680 (2000).
 - ⁵ M. Saba, C. Ciuti, J. Bloch, V. Thierry-Mieg, R. Andre, Le Si Dang, S. Kundermann, A. Mura, G. Bongiovanni, J. L. Staehli, et al., *Nature* **414**, 731 (2001).
 - ⁶ D. M. Whittaker, *Phys. Rev. B* **63**, 193305 (2001).
 - ⁷ C. Ciuti, P. Schwendimann, and A. Quattropani, *Semicond. Sci. Technol.* **18**, 279 (2003).
 - ⁸ J. J. Baumberg and P. G. Lagoudakis, *Phys. Stat. Sol. (b)* **242**, 2210 (2005).
 - ⁹ J. Keeling, F. M. Marchetti, M. H. Szymanska, and P. B. Littlewood, *Semicond. Sci. Technol.* **22**, R1 (2007).
 - ¹⁰ P. G. Lagoudakis, P. G. Savvidis, J. J. Baumberg, D. M. Whittaker, P. R. Eastham, M. S. Skolnick, and J. S. Roberts, *Phys. Rev. B* **65**, 161310(R) (2002).
 - ¹¹ A. Kavokin, P. G. Lagoudakis, G. Malpuech, and J. J. Baumberg, *Phys. Rev. B* **67**, 195321 (2003).
 - ¹² P. R. Eastham and D. M. Whittaker, *Phys. Rev. B* **68**, 075324 (2003).
 - ¹³ P. Renucci, T. Amand, X. Marie, P. Senellart, J. Bloch, B. Sermage, and K. V. Kavokin, *Phys. Rev. B* **72**, 075317 (2005).
 - ¹⁴ K. V. Kavokin, P. Renucci, T. Amand, X. Marie, P. Senellart, J. Bloch, and B. Sermage, *Phys. Stat. Sol. (c)* **2**, 763 (2005).
 - ¹⁵ G. Dasbach, C. Diederichs, J. Tignon, C. Ciuti, Ph. Roussignol, C. Delalande, M. Bayer, and A. Forchel, *Phys. Rev. B* **71**, 161308(R) (2005).
 - ¹⁶ D. N. Krizhanovskii, D. Sanvitto, I. A. Shelykh, M. M. Glazov, G. Malpuech, D. D. Solnyshkov, A. Kavokin, S. Ceccarelli, M. S. Skolnick, and J. S. Roberts, *Phys. Rev. B* **73**, 073303 (2006).
 - ¹⁷ S. Schumacher, N. H. Kwong, and R. Binder, *Phys. Rev. B*, in press, arXiv.org:cond-mat/0708.1194v1 **76** (2007).
 - ¹⁸ D. Sanvitto, D. N. Krizhanovskii, S. Ceccarelli, M. S. Skolnick, and J. S. Roberts, *Physica E* **32**, 492 (2006).
 - ¹⁹ L. Klotkowski, M. D. Martin, A. Amo, L. Vina, I. A. Shelykh, M. M. Glazov, G. Malpuech, A. V. Kavokin, and R. Andre, *Solid State Communications* **139**, 511 (2006).
 - ²⁰ M. D. Martin, G. Aichmayr, A. Amo, D. Ballarini, L. Klotkowski, and L. Vina, *J. Phys.: Condens. Matter* **19**, 295204 (2007).
 - ²¹ M. Romanelli, C. Leyder, J. Ph. Karr, E. Giacobino, and A. Bramati, *Phys. Rev. Lett.* **98**, 106401 (2007).
 - ²² N. H. Kwong, R. Takayama, I. Rumyantsev, M. Kuwata-Gonokami, and R. Binder, *Phys. Rev. B* **64**, 045316 (2001).
 - ²³ N. H. Kwong, R. Takayama, I. Rumyantsev, M. Kuwata-Gonokami, and R. Binder, *Phys. Rev. Lett.* **87**, 027402 (2001).
 - ²⁴ S. Savasta, O. Di Stefano, and R. Girlanda, *Phys. Rev. Lett.* **90**, 096403 (2003).
 - ²⁵ S. Schumacher, N. H. Kwong, and R. Binder, submitted, arXiv.org:cond-mat/0708.0442v1 (2007).
 - ²⁶ M. Wouters and I. Carusotto, *Phys. Rev. B* **75**, 075332 (2007).
 - ²⁷ N. A. Gippius, I. A. Shelykh, D. D. Solnyshkov, S. S. Gavrilov, Y. G. Rubo, A. V. Kavokin, S. G. Tikhodeev, and G. Malpuech, *Phys. Rev. Lett.* **98**, 236401 (2007).
 - ²⁸ W. Langbein, I. Shelykh, D. Solnyshkov, G. Malpuech, Y. Rubo, and A. Kavokin, *Phys. Rev. B* **75**, 075323 (2007).
 - ²⁹ A. Kavokin, G. Malpuech, and M. Glazov, *Phys. Rev. Lett.* **95**, 136601 (2005).
 - ³⁰ C. Diederichs, J. Tignon, G. Dasbach, C. Ciuti, A. Lemaitre, J. Bloch, P. Roussignol, and D. Delalande, *Nature* **440**, 904 (2006).
 - ³¹ S. Schumacher, N. H. Kwong, and R. Binder, submitted, arXiv.org:cond-mat/0708.1300v1 (2007).